Accepted Manuscript

Degradation of tri(2-chloroisopropyl) phosphate by the UV/H_2O_2 system: Kinetics, mechanisms and toxicity evaluation

Huan He, Qiuyi Ji, Zhanqi Gao, Shaogui Yang, Cheng Sun, Shiyin Li, Limin Zhang

PII: S0045-6535(19)31609-1

DOI: https://doi.org/10.1016/j.chemosphere.2019.124388

Article Number: 124388

Reference: CHEM 124388

To appear in: *ECSN*

Received Date: 24 March 2019

Revised Date: 15 July 2019

Accepted Date: 16 July 2019

Please cite this article as: He, H., Ji, Q., Gao, Z., Yang, S., Sun, C., Li, S., Zhang, L., Degradation of tri(2-chloroisopropyl) phosphate by the UV/H_2O_2 system: Kinetics, mechanisms and toxicity evaluation, *Chemosphere* (2019), doi: https://doi.org/10.1016/j.chemosphere.2019.124388.

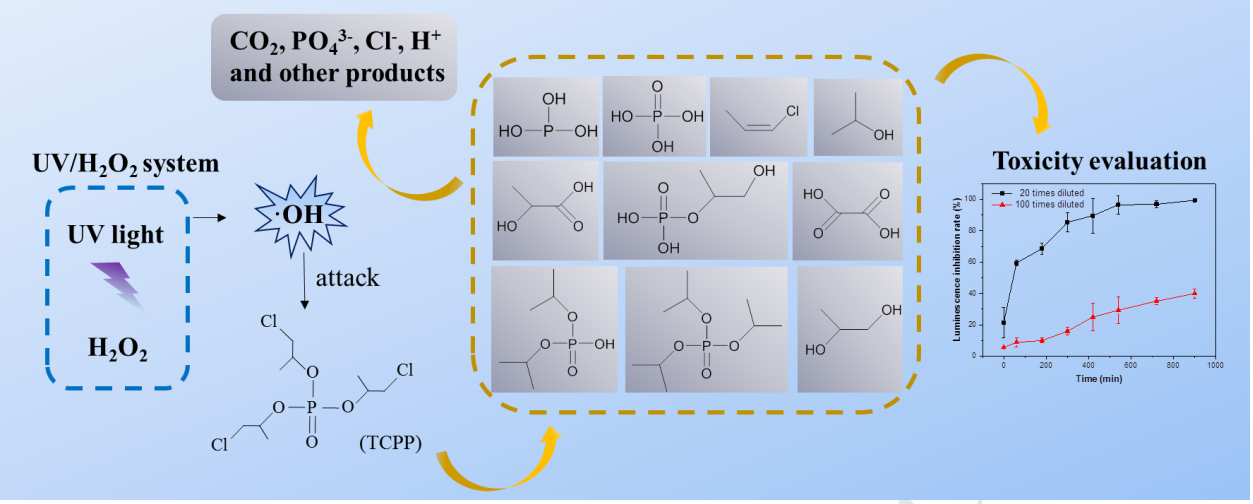

Degradation of tri(2-chloroisopropyl) phosphate by the UV/H_2O_2 system: kinetics, mechanisms and toxicity evaluation

Huan He[1], Qiuyi Ji[1], Zhanqi Gao[2], Shaogui Yang[1*], Cheng Sun[3], Shiyin Li[1], Limin Zhang[1]

[1]*School of Environment, Nanjing Normal University, Nanjing, Jiangsu 210023, P.R. China*

[2]*State Environmental Protection Key Laboratory of Monitoring and Analysis for Organic Pollutants in Surface Water, Environment Monitoring Center of Jiangsu Province, Nanjing 210036, P.R. China*

[3] *State Key Laboratory of Pollution Control and Resources Reuse, School of Environment, Nanjing University, Nanjing, Jiangsu 210023, P.R. China*

Abstract: A photodegradation technology based on the combination of ultraviolet radiation with H_2O_2 (UV/H_2O_2) for degrading tri(chloroisopropyl) phosphate (TCPP) was developed. In ultrapure water, a pseudo-first order reaction was observed, and the degradation rate constant reached 0.0035 min^{-1} (R^2=0.9871) for 5 mg L^{-1} TCPP using 250 W UV light irradiation with 50 mg L^{-1} H_2O_2. In detail, the yield rates of Cl^- and PO_4^{3-} reached 0.19 mg L^{-1} and 0.58 mg L^{-1}, respectively. The total organic carbon (TOC) removal rate was 43.02%. The pH value of the TCPP solution after the reaction was 3.46. The mass spectrometric detection data showed a partial transformation of TCPP into a series of hydroxylated and dechlorinated products. Based on the luminescent bacteria experimental data, the toxicity of TCPP products increased obviously as the reaction proceeded. In conclusion, degradation of high concentration TCPP in UV/H_2O_2 systems may result in more toxic substances, but its potential application for real wastewater is promising in the future after appropriate optimization, domestication and evaluation.

Key words : TCPP, UV/H_2O_2, kinetics, mechanisms, toxic evaluation

[*] Corresponding author. Tel.: +86 25 85891849, Fax: +86 25 85891849
E-mail addresses: yangsg@njnu.edu.cn (SG Yang)

1. Introduction

Emerging contaminants (ECs) are defined as chemicals that have recently been detected in the environment, which pose a significant risk to human and ecosystem health. The ECs mainly include personal care products, pharmaceuticals, pesticides and disinfectants, etc. (Montes et al., 2015). An important class of ECs are flame retardants (FRs). The materials processed by the FRs can effectively prevent, delay or terminate the propagation of the flame when attacked by external fire sources, thereby achieving the flame retarding effect. Phosphorus flame retardants (PFRs), which have been used for over 150 years, can be divided into three main groups (Veen and Boer, 2012): organophosphate esters (OPEs), phosphonates, and phosphinates. The existing studies are focused mainly on tetrabromobisphenol A and other polybrominated diphenyl ethers (PBDEs) (Chow et al., 2012; Chunyan et al., 2012; Guo et al., 2012; Huang et al., 2013; Cao et al., 2015). However, the research data of organophosphorus (OPFRs) is very scarce (Antonopoulou et al., 2016).

OPEs are not chemically bound in materials and easily leach into the environment via abrasion, volatilization and dissolution. As a result, OPEs have been frequently detected in the environment, such as seawater and groundwater and increasingly in indoor environments (Andresen et al., 2004; Axel et al., 2011). Tri(chloroisopropyl) phosphate (TCPP), one of chlorinated organophosphate esters (Cl-OPEs), represents approximately 80% of the chlorinated OPFRs in Europe and is by volume the most important OPFR (Bollmann et al., 2012). Recent studies have reported that TCPP is among the most frequently detected emerging pollutants in wastewater effluents in EU at concentration as high as 24 μg L^{-1}. TCPP has been also detected in surface water, ground water and drinking water reaching concentrations ranging from few ng L^{-1} to few μg L^{-1}, even mg L^{-1} in wastewater (Bollmann et al., 2012; Cristale et al., 2013; Jun et al., 2014). Physical, biological and

chemical treatment methods have been used to remove the Cl-OPEs. Adsorbents such as modified zeolites (Grieco and Ramarao, 2013) and carbon nanotubes (Yan and Jing, 2014) can effectively adsorb chlorinated organophosphates in water, but cannot achieve the purpose of degradation or mineralization of Cl-OPEs. The biological method has a low removal rate of the Cl-OPEs. Only 12.3% of tri(2-chloroethyl)phosphate (TCEP) and 11.8% of TCPP can be removed in the University of Capetown (UCT) process (Pang et al., 2016). Among treatment methods, the advanced oxidation processes (AOPs) in chemical treatment method are one of the most effective methods for degrading Cl-OPEs (Watts and Linden, 2009).

The AOPs, including electrochemistry (Loffler et al., 2019), ozonation (Dar et al., 2019), sonolysis (Choi et al., 2019), UV/H_2O_2 photolysis (Qiu et al., 2019), photocatalysis (Monteagudo et al., 2019), and Fenton process (Rostamizadeh et al., 2019), are the most commonly used chemical methods for water treatment. The potential application of ultraviolet-advanced oxidation processes (UV-AOPs) to the degradation of OPEs has only begun in recent years. Yuan et al. (2015) have found that UV/H_2O_2 was more efficient than ozonation for the degradation of OPEs in a municipal secondary effluent. The UV/H_2O_2 process is a conventional advanced oxidation process, based on the production of hydroxyl radicals (•OH) via the photolysis of H_2O_2. The hydroxyl radicals (•OH) are extraordinarily reactive and can attack most organic molecules with very high rate constants (Andreozzi et al., 1999). Thus, the hydroxyl radicals (•OH) can degrade rapidly and non-selectively a wide range of organic pollutants in aquatic environment (Khataee et al., 2009). The quantum yield of •OH production and molar absorption coefficient of H_2O_2 at 254 nm were 0.5 mol E^{-1} and 18.6 $M^{-1}cm^{-1}$, respectively (Morgan et al., 1988; Liao and Gurol, 1995). Hence, the UV/H_2O_2 process has been confirmed to be effective in degrading organic pollutants in aquatic environments (Bledzka et

al., 2010; Ghodbane and Hamdaoui, 2010; Pamela et al., 2010; Zhou et al., 2012).

The removal of OPEs in the UV/H_2O_2 system has been reported in the literature (Santoro et al., 2010), but the bis(trimethylsilyl)trifluoroacetamide (BSTFA) derivatization and quantum calculations are still unclear. Gas chromatography mass spectrometry (GC-MS) and nuclear magnetic resonance are often used as means of mechanism analysis, but the identification of intermediates requires verification by quantum calculations (Watts and Linden, 2008). Previous studies have carried out research on low concentration Cl-OPEs, but there are few studies on high concentration Cl-OPEs. There is still a knowledge gap on the detailed mechanisms and pathways involving the degradation of TCPP using UV/H_2O_2, not to mention the environmental safety of their degradation products. Besides, the degradation pathway of TCPP in the UV/H_2O_2 system has not been reported yet and the toxicity of the intermediates and the toxicity of the degradation system require further investigation.

The present study aims to degrade high concentration TCPP in the UV/H_2O_2 system and perform the kinetics, mechanisms and toxicity analysis. Besides, it also aims to identify the toxic intermediates of TCPP during its degradation. The intermediates were identified by GC–MS. Quantum calculation was also carried out to ascertain the position of the TCPP molecule where the oxidation was firstly initiated. The degradation pathway was estimated based on the intermediate product. In addition, the toxicity of the intermediates was consulted and the toxicity of the degradation system was evaluated by luminescent bacteria experiments.

2. Experimental section

2.1. Chemicals

The TCPP was purchased from Aldrich (Milwaukee, WI, USA). H_2O_2 (30%, v/v) was obtained

from Fisher Company. HPLC-grade methanol, ethyl acetate, acetonitrile and dimethysulphoxide (DMSO) were purchased from Tedian Company and used without further purification. The luminescent bacteria *Photobacterium phosphoreum T3* (*P. phosphoreum*, Strain Number CS233) was obtained as freeze-dried reagents (0.5 g each bottle) from the Institute of Soil Science, Chinese Academy Sciences, Nanjing, China. They were stored at -20 □ and hydrated prior to testing. Ultrapure deionized water was obtained from a Milli-Q water purification system (Milli-Q system, Millipore, Beldford, MA) and was used in the preparation of all the aqueous solution.

2.2. Experimental Procedures

The degradation experiments were carried out in a photoreactor (XPA-7, Xujiang Power Plant, Nanjing, China). XPA-7 multi-tube stirring reaction instrument (Fig. S2) includes light source, quartz cold trap, quartz test tube, reaction vessel, multi-tube stirring device, rotating device, water tank, micro water pump, light shield, etc. Samples can be magnetically stirred and evenly illuminated in a test tube with a uniform rotation around the light source. The UV lamps (250 W) were manufactured by Shanghai Yaming Lighting Co., Ltd., China. The emitted UV-light flux was measured by an actinometer made by Beijing Normal University (Beijing, China). Solutions spiked with 5 mg L^{-1} of target compound and 50 mg L^{-1} H_2O_2 (30%) were irradiated while continuously mixed. The total solution volume for each exposure was 50 mL.

2.3. Analytical methods

The residual TCPP was extracted from 1 mL of the UV-H_2O_2 treated solution with 1 mL of ethyl acetate by a mixture of liquid and liquid mixture. The extracted analytes were then separated and assayed by a 7890N gas chromatograph (Agilent Technologies, USA) equipped with a split/splitless injector, HP-5 capillary column (30 m x 0.32 mm i.d., 0.25 μm film thickness) and flame

Photometric detector (FPD). The column temperature was set as follows: the initial oven temperature was 80 °C (for 1 minute), the temperature was raised to 140 °C at a rate of 20 °C min^{-1} (for 2 min), and then increased at a rate of 4 °C min^{-1} up to 280 °C (for 6 min). The injector and detector temperatures were set at 250 °C. Helium (99.999%) was used as a carrier gas at a constant flow rate of 1.5 mL min^{-1} and nitrogen (99.999%) was used as a make-up gas at a flow rate of 20 mL min^{-1}. Synthetic air (99.995%) and hydrogen (99.999%) were used as detector gases at flow rates of 100 and 65 mL min^{-1}, respectively.

Due to the complexity of the intermediate product, the Thermo Fisher Trace gas chromatograph coupled to a Polaris Q ion trap mass spectrometer (GC/MS, Thermo Fisher, USA) with a DB-5 fused silica capillary column (30 m, 0.32 mm i.d., 0.25 mm film thickness) was used to analyze the sample. Samples were extracted by SPE column Poly-Sery PSD prior to GC-MS analysis.

All SPE columns were sequentially adjusted with 5 mL of methanol and water at a flow rate of 1 mL min^{-1} prior to use. The loaded SPE column was then eluted with 5 mL acetonitrile / ethyl acetate (1:1, V/V). The extracted solution was dried over anhydrous sodium sulfate and concentrated to 1 mL by rotary evaporation. After the solvent was purged with mild nitrogen, trimethylsilylation was carried out with 0.2 mL of BSTFA at 60 °C for 15 h. The initial temperature of the column oven was 40 °C, and after maintaining at this temperature for 1 minute, it was then heated to 300 °C at a heating rate of 6 °C min^{-1}. Helium was used as a carrier gas. Mass spectrometry was performed in a 70 eV electron bombardment (EI) mode. Electron impact was used for ionization of the sample. Some intermediates were identified by the National Institute of Standards and Technology (NIST) library identification process.

2.4. Calculation of the Frontier electron density and bond dissociation enthalpies (BDEs)

The ab initio molecular orbital (MO) calculations were carried out using Gaussian 03 program (Gaussian, Inc.). Structures were fully optimized with the B3LYP/6-311+G* basis set at the level of the density functional theory (DFT) for all calculations. Then, the Frontier electron densities (FEDs) of the highest occupied molecular orbital (HOMO) and the lowest unoccupied molecular orbital (LUMO) were calculated.

2.5. Toxicity measurements

For the acute toxicity tests, 200 mL of solution before or after reduction/oxidation treatment was collected. The pH values of all samples were adjusted to 7.0 before the toxicity test. The water samples were filtered through membrane filter with a porosity of 0.45 μm, and then passed through a column with non-polar neutral resin (XAD-2). The constituents adsorbed on the column and the filtered nanoparticles were eluted by methanol, acetone and dichloromethane. The elution was concentrated to 1 mL by rotary evaporation, dried by the gentle nitrogen and then re-dissolved in 1 mL DMSO. Finally, the samples were stored at −18 ◦C in the dark. Prior to toxicity assessment, the bacteria *P. phosphoreum* was reactivated in 1 mL 2.5% NaCl solution and stored in an ice water bath. Subsequently, 0.2 mL of each treated sample and 10 μL reactivated bacteria were added to 2 mL of 3% NaCl solution. After being exposed to sample for 15 min at 15±1 °C, the bioluminescence was measured by the DeltaTox Analyzer (SDI, USA). DMSO was used as solvent control. Each degradation reaction sample of TCPP was run in duplicate set. Toxicity was expressed as the luminescence inhibition ratio and it could be described as Eq. 1:

$$\text{Inhibition rate (\%)} = (1 - \frac{\text{Sample intensity}}{\text{Control intensity}}) \times 100\% \qquad \text{(Eq. 1)}$$

3. Results and discussion

3.1. Performance of TCPP degradation by UV/H_2O_2 system

Photolysis of H_2O_2 was the predominant mode of •OH formation. Hydroxyl radical, with its relatively high redox potential (2.8 V), is often the oxidant of choice for engineered remediation of waters pollutants. The potential for •OH formation in UV-irradiated water containing the oxidant H_2O_2 has led to the design and implementation of UV/H_2O_2 for oxidation of unwanted organics at full-scale water treatment plants. The results in Fig.S1 indicated that no obvious removal of the TCPP was observed in the UV alone experiment, due to its poor UV absorbance properties in the UV-C range (λ=200–300 nm). Therefore, at an initial concentration of 50 mg L^{-1}, H_2O_2 was the only significant photon absorber (λ=254 nm) in irradiated solutions. As shown in Fig.1, the degradation of the TCPP approximately followed the pseudo-first-order reaction in kinetics under tested conditions. The pseudo-first-order rate constant k was measured for the oxidation rate of TCPP, which was 0.0035 min^{-1} (R^2=0.9871).

TCPP is composed of carbon, hydrogen, oxygen, chlorine, and phosphorus elements. Therefore, the final degradation products of TCPP should contain CO_2, H^+, Cl^- and PO_4^{3-}. The simplified oxidation pathway for TCPP in the UV/H_2O_2 system can be described as Eq. 2:

$$C_9H_{18}Cl_3PO_4 \xrightarrow{\text{Oxidation}} CO_2 + H^+ + Cl^- + PO_4^{3-} + \text{Intermediates} \qquad \text{(Eq. 2)}$$

The final product of TCPP in the UV/H_2O_2 system included Cl^-, PO_4^{3-}, CO_2 and H^+. The concentrations of Cl^- and PO_4^{3-} after photooxidation were measured to evaluate the degradation efficiency of TCPP. Besides, the TOC and pH values were also measured.

3.2. TOC, pH, Cl^- and PO_4^{3-} analysis

3.2.1 TOC removal rate and pH values of TCPP aqueous solution in the UV/H_2O_2 system

TOC values before and after photooxidation were measured to evaluate the mineralization effect of TCPP. A Shimadzu TOC-5000A TOC (combustion) analyzer was employed to evaluate the

mineralization efficiency of target compounds. The removal rate of TOC can be expressed as TOC (%). In ambient temperature, the reaction time from 0 to 900 min were examined. It can be seen from Fig. 2A that the TOC removal increased with the increasing of reaction time from 0 to 900 min. From 720 min to 900 min, the rate of increase in TOC removal rate was significantly faster. At 900 min, the removal rate of TOC reached up to 43.02%, indicating that the UV/H_2O_2 system had a certain effect on the degradation of TCPP.

The pH values of the system were measured by suppression of the eluent and achieved with a Dionex anion ASRS 300 electrolytic suppressor (4 mm) in the auto suppression external water mode. The pH values after the reaction were depicted in Fig. 2B. From 0 to 180 min, the pH value of TCPP began to show sharp drops, after that (from 180 min to 900 min) the pH value changed unremarkably. The initial pH value of TCPP was 8.02 and final pH value was 3.46, indicating that there was a large amount of H^+ production in the UV/H_2O_2 system, further confirming that TCPP was degraded.

3.2.2 Concentration of Cl^- and PO_4^{3-} of TCPP aqueous solution in the UV/H_2O_2 system

The final degradation products of TCPP are supposed to include Cl^- and PO_4^{3-}. The residual concentration of Cl^- and PO_4^{3-} can be employed to evaluate the degradation of organic contaminants. The concentration of Cl^- and PO_4^{3-} in the UV/H_2O_2 system can indicate the degradation degree of TCPP. The formation of Cl^- and PO_4^{3-} in the UV/H_2O_2 system was analyzed by a Dionex ion chromatograph (IC, Dionex model ICS 1000) equipped with a dual-piston (in series) pump, a Dionex IonPac AS11-HC analytical column (4 mm, 250 mm) and a Dionex DS6 conductivity detector.

From Fig. 2C and 2D, it is obvious that the concentration of Cl^- and PO_4^{3-} increases with the

increase of the time from 0 to 900 min. The theoretical concentration of Cl^- and PO_4^{3-} was 1.63 mg L^{-1} and 1.45 mg L^{-1}, respectively. The formation concentration of Cl^- and PO_4^{3-} was 0.19 mg L^{-1} and 0.58 mg L^{-1}. That is, the degradation rate of Cl^- and PO_4^{3-} was 11.7% and 40%. The low degradation rate of Cl means the formation of chlorine-containing compounds, which may cause the solution to be highly toxic after degradation. The results obtained may also be related to the bond energy.

3.3. Calculation of the frontier electron densities (FEDs) and bond dissociation enthalpies (BDEs)

The ab initio molecular orbital (MO) calculations were carried out using Gaussian 03 program (Gaussian, Inc.). Structures were fully optimized with the B3LYP/6-311+G* basis set at the level of the density functional theory (DFT) for all calculations. Then, the FEDs of the highest occupied molecular orbital (HOMO) and the lowest unoccupied molecular orbital (LUMO) were calculated. The values of $FED_{HOMO}^2 + FED_{LUMO}^2$ were obtained to predict the reaction sites for radical attack. The C-H BDEs and O-H BDEs were also calculated to predict the reaction sites for abstracting hydrogen reaction initiated by hydroxyl radical. From Table 1, the larger the value of $2FED_{HOMO}^2$, the higher the density of the electron cloud, and the easier it is to be attacked by •OH, such as C9 (0.344), C15 (0.591) and Cl 16 (0.349). The larger the value of $FED_{HOMO}^2 + FED_{LUMO}^2$, the stronger the activity of the reaction, which means that it is unstable and prone to reaction, such as P1 (0.888). From Table 2, the smaller the bond energy, the more unstable it is, such as P1-O8 (0.6216) and C9-C15 (0.6844).

3.4. Degradation pathways of TCPP

The degradation of TCPP mainly included two pathways (Fig. 3). The first pathway included 4 routes. Route I was an •OH addition reaction and a hydrogen extraction reaction to form

1-chloropropan-2-ol. In route II, Compound 1 was produced by 1-chloropropan-2-ol with dehydration. Compound 2 was generated by the •OH addition reaction, oxidized to Compound 3, and further oxidized to Compound 4. Compound 7 was produced by 1-chloropropan-2-ol with hydrogen abstraction. Compound 5 was generated by hydrogen extraction reaction and Compound 6 was further generated by •OH addition in route III. Route IV generated oxygen by oxidation of H_2O_2 and generated Compound 8 by the addition reaction of •OH. The second pathway generated 1-chloropropan-2-yl dihydrogen phosphate by the addition reaction of •OH and H_2O, and generated Compound 11 by attacking C11-Cl 12 and C15-Cl 16 by •OH. 1-chloropropan-2-yl dihydrogen phosphate generated Compound 9 and Compound 10 by attacking P1-O3 and C5-Cl 6 by •OH, respectively. From Table 3, the LC_{50} of Compound 1 is 221 mg L^{-1}, which is much more toxic than TCPP (LD_{50}=1500 mg kg^{-1}, Wikipedia). Since the pH value was adjusted to 7.0 before the toxicity test, the effect of hydrogen ions can be ignored. According to the removal rate of the TOC (Fig. 2A), it can be known that about 57% of the organic molecules were not converted to CO_2. From the calculation of the theoretical and actual values of chloride ions (Fig. 2C) and the degradation rate of TCPP (Fig. 1), it can be inferred that the intermediates produced chlorine-containing compounds. When luminescent bacteria are used to detect toxicity, a high concentration of salt must be added to the test system to maintain their normal survival. Therefore, an increase in the concentration of chloride ions (Fig. 2C) did not affect the toxicity test. Hence, the toxicity was the result of a combination of various products or components in the degradation process.

3.5. Toxicity evaluation

The luminescent bacteria toxicity test can effectively detect the acute toxicity of intermediate products. When these bacteria were in a toxic environment, the light they emit would be suppressed.

The toxicity of the sample can be quickly and accurately tested according to the change in light intensity, and the potential toxic substances can be directly detected. That is to say, the higher the luminescence inhibition rate, the greater the toxicity of the aqueous solution sample. It can be seen from Fig.4 that as the reaction time increases, the luminescence inhibition rate of the TCPP diluted 20 times and diluted 100 times in the system gradually increases, that is, the toxicity of intermediate products gradually increases. TCPP has less toxicity studies, but its acute toxicity is smaller than TCEP, so it has been used as a substitute for TCEP. The LD_{50} of TCPP is 1500 mg kg^{-1} and the LC_{50} of Compound 1 is 221 mg L^{-1}. The intermediate product Compound 1 and other compounds with unknown toxicity produced by degradation may be the main cause of high toxicity. Among the detected intermediates, Compound 1 was the only chlorine-containing compound. Since the pH was adjusted to 7.0 before the toxicity test, the inhibitory effect of H^+ on the luminescent bacteria can be excluded. Chloride ion was a salt necessary for luminescent bacteria, so it did not inhibit the illumination intensity. Based on the results of incomplete removal of the TOC, it was concluded that Compound 1 was able to influence the toxicity of the solution to a large extent. As is known to all, Cl-containing compounds are highly toxic. Thus, in order to reduce the toxicity of aqueous solution, how to remove Cl-containing compounds from water should be taken into consideration in the next step. For example, a nanofiltration reverse osmosis unit can be added to the UV/H_2O_2 system. Yujia et al. (2019) have found that the early stage products have lower toxicity than TCEP (initial concentration was 3.51 μM) or their further small molecule products with 185 nm vacuum ultraviolet based on the toxicology analysis including reactive oxygen species and apoptosis of *Escherichia coli*. Based on the proteomics data at molecular and metabolic network levels, the toxicity of TCEP (initial concentration was 3.5 μM) products was reduced obviously as the reaction

proceeded (Liu et al., 2018), which was different from the research results of this paper. The main reason may be that the initial concentration of TCPP in this paper was high (5 mg L^{-1}), the reaction time was not long enough, so the point of toxicity reduction has not yet been reached.

4. Conclusions

The degradation rate of 5 mg L^{-1} TCPP in UV/H_2O_2 system can reach 96% in 900 min. The degradation of TCPP using UV/H_2O_2 followed a pseudo-first order reaction with a k of 0.0035 min^{-1} (R^2=0.9871) and •OH was confirmed to be the dominating active radical species. As the reaction proceeded, TCPP was transformed to several hydroxylated and dechlorinated products. Based on the luminescent bacteria experimental data, the toxicity of TCPP products was increased obviously as the reaction proceeded. In conclusion, degradation TCPP at a high concentration (5 mg L^{-1}) in UV/H_2O_2 systems may result in more toxic substances, but its potential application for real wastewater is promising in the future after appropriate optimization, domestication and evaluation. For example, a nanofiltration reverse osmosis unit can be introduced to the UV/H_2O_2 system.

Acknowledgments

This research was supported jointly by the National Nature Science Foundation of China (No. 21777067), the Six Talent Peaks Project in Jiangsu Province (No. JNHB-105), National water pollution control and treatment technology major special subject (No. 2017ZX07202004), the Open Fund of the State Environmental Protection Key Laboratory of Wetland Ecology and Vegetation Restoration, Northeast Normal University (No. 130028903) and Introducing Talent Research Start-up Project of Nanjing Normal University.

References

Andreozzi, R., Caprio, V., Insola, A., Marotta, R., 1999. Advanced oxidation processes (AOP) for water purification and recovery. Catal. Today 53, 51-59.

Andresen, J.A., Grundmann, A., Bester, K., 2004. Organophosphorus flame retardants and plasticisers in surface waters. Sci. Total Environ. 332, 155-166.

Antonopoulou, M., Karagianni, P., Konstantinou, I.K., 2016. Kinetic and mechanistic study of photocatalytic degradation of flame retardant Tris (1-chloro-2-propyl) phosphate (TCPP). Appl. Catal. B-Environ. 192, 152-160.

Axel, M.L., Zhiyong, X., Armando, C., Renate, S., Ralf, E., 2011. Organophosphorus flame retardants and plasticizers in the atmosphere of the North Sea. Environ. Pollut. 159, 3660-3665.

Bledzka, D., Gryglik, D., Olak, M., Gebicki, J.L., Miller, J.S., 2010. Degradation of n-butylparaben and 4-tert-octylphenol in H_2O_2/UV system. Radiat. Phys. Chem. 79, 409-416.

Bollmann, U.E., Möller, A., Xie, Z., Ebinghaus, R., Einax, J.W., 2012. Occurrence and fate of organophosphorus flame retardants and plasticizers in coastal and marine surface waters. Water Res. 46, 531-538.

Cao, M., Wang, P., Ao, Y., Chao, W., Hou, J., Jin, Q., 2015. Photocatalytic degradation of tetrabromobisphenol A by a magnetically separable graphene–TiO_2 composite photocatalyst: Mechanism and intermediates analysis. Chem. Eng. J. 264, 113-124.

Choi, C.H., Ko, D.H., Park, B., Choi, Y., Choi, W., Kim, D.P., 2019. Air-water interfacial fluidic sonolysis in superhydrophobic silicon-nanowire-embedded system for fast water treatment. Chem. Eng. J. 358, 1594-1600.

Chow, K.L., Man, Y.B., Zheng, J.S., Liang, Y., Tam, N.F.Y., Wong, M.H., 2012. Characterizing the optimal operation of photocatalytic degradation of BDE-209 by nano-sized TiO_2. J. Environ. Sci. 24, 1670-1678.

Chunyan, S., Jincai, Z., Hongwei, J., Wanhong, M., Chuncheng, C., 2012. Photocatalytic debromination of preloaded decabromodiphenyl ether on the TiO_2 surface in aqueous system. Chemosphere 89, 420-425.

Cristale, J., García, V.A., Barata, C., Lacorte, S., 2013. Priority and emerging flame retardants in rivers: Occurrence in water and sediment, Daphnia magna toxicity and risk assessment. Environ. Int. 59, 232-243.

Dar, A.A., Wang, X.H., Wang, S.Y., Ge, J.L., Shad, A., Ai, F.X., Wang, Z.Y., 2019. Ozonation of pentabromophenol in aqueous basic medium: Kinetics, pathways, mechanism, dimerization and toxicity assessment. Chemosphere 220, 546-555.

Ghodbane, H., Hamdaoui, O., 2010. Decolorization of antraquinonic dye, C.I. Acid Blue 25, in aqueous solution by direct UV irradiation, UV/H_2O_2 and UV/Fe(II) processes. Chem. Eng. J. 160, 226-231.

Grieco, S.A., Ramarao, B.V., 2013. Removal of TCEP from aqueous solutions by adsorption with zeolites. Colloid Surface A. 434, 329-338.

Guo, Y., Lou, X., Xiao, D., Xu, L., Wang, Z., Liu, J., 2012. Sequential reduction–oxidation for photocatalytic degradation of tetrabromobisphenol A: Kinetics and intermediates. J. Hazard. Mater. 241-242, 301-306.

Huang, A.Z., Wang, N., Lei, M., Zhu, L.H., Zhang, Y.Y., Lin, Z.F., Yin, D.Q., Tang, H.Q., 2013. Efficient Oxidative Debromination of Decabromodiphenyl Ether by TiO_2-Mediated

Photocatalysis in Aqueous Environment. Environ. Sci. Technol. 47, 518-525.

Jun, L., Nanyang, Y., Beibei, Z., Ling, J., Meiying, L., Mengyang, H., Xiaowei, Z., Si, W., Hongxia, Y., 2014. Occurrence of organophosphate flame retardants in drinking water from China. Water Res. 54, 53-61.

Khataee, A.R., Vatanpour, V., Ghadim, A.R.A., 2009. Decolorization of C.I. Acid Blue 9 solution by UV/Nano-TiO_2, Fenton, Fenton-like, electro-Fenton and electrocoagulation processes: A comparative study. J. Hazard. Mater. 161, 1225-1233.

Liao, C.H., Gurol, M.D., 1995. Chemical oxidation by photolytic decomposition of hydrogen peroxide. Environ. Sci. Technol. 29, 3007-3014.

Liu, J., Ye, J., Chen, Y., Li, C., Ou, H., 2018. UV-driven hydroxyl radical oxidation of tris(2-chloroethyl) phosphate: Intermediate products and residual toxicity. Chemosphere 290, 225-233.

Loffler, T., Clausmeyer, J., Wilde, P., Tschulik, K., Schuhmann, W., Ventosa, E., 2019. Single entity electrochemistry for the elucidation of lithiation kinetics of TiO_2 particles in non-aqueous batteries. Nano Energy 57, 827-834.

Monteagudo, J.M., Duran, A., San Martin, I., Carrillo, P., 2019. Effect of sodium persulfate as electron acceptor on antipyrine degradation by solar TiO_2 or TiO_2/rGO photocatalysis. Chem. Eng. J. 364, 257-268.

Montes, N., Otero, M., Coimbra, R.N., Méndez, R., Martínvillacorta, J., 2015. Removal of tetracyclines from swine manure at full-scale activated sludge treatment plants. Environ. Technol. 36, 1966-1973.

Morgan, M.S., Trieste, P.F.V., Garlick, S.M., Mahon, M.J., Smith, A.L., 1988. Ultraviolet molar

absorptivities of aqueous hydrogen peroxide and hydroperoxyl ion. Anal. Chim. Acta 215, 325-329.

Pamela, C.A., Mohamed Gamal, E.D., Smith, D.W., 2010. Degradation of bromoxynil and trifluralin in natural water by direct photolysis and UV plus H_2O_2 advanced oxidation process. Water Res. 44, 2221-2228.

Pang, L., Yang, P.J., Zhao, J.H., Zhang, H.Z., 2016. Comparison of wastewater treatment processes on the removal efficiency of organophosphate esters. Water Sci. Technol. 74, 1602-1609.

Qiu, W.H., Zheng, M., Sun, J., Tian, Y.Q., Fang, M.J., Zheng, Y., Zhang, T., Zheng, C.M., 2019. Photolysis of enrofloxacin, pefloxacin and sulfaquinoxaline in aqueous solution by UV/H_2O_2, UV/Fe(II), and UV/H_2O_2/Fe(II) and the toxicity of the final reaction solutions on zebrafish embryos. Sci. Total Environ. 651, 1457-1468.

Rostamizadeh, M., Jalali, H., Naeimzadeh, F., Gharibian, S., 2019. Efficient Removal of Diclofenac from Pharmaceutical Wastewater Using Impregnated Zeolite Catalyst in Heterogeneous Fenton Process. Phys. Chem. Res. 7, 37-52.

Santoro, D., Raisee, M., Moghaddami, M., Ducoste, J., Sasges, M., Liberti, L., Notarnicola, M., 2010. Modeling Hydroxyl Radical Distribution and Trialkyl Phosphates Oxidation in UV-H_2O_2 Photoreactors Using Computational Fluid Dynamics. Environ. Sci. Technol. 44, 6233-6241.

Veen, I.V.D., Boer, J.D., 2012. Phosphorus flame retardants: Properties, production, environmental occurrence, toxicity and analysis. Chemosphere 88, 1119-1153.

Watts, M.J., Linden, K.G., 2008. Photooxidation and subsequent biodegradability of recalcitrant tri-alkyl phosphates TCEP and TBP in water. Water Res. 42, 4949-4954.

Watts, M.J., Linden, K.G., 2009. Advanced Oxidation Kinetics of Aqueous Trialkyl Phosphate

Flame Retardants and Plasticizers. Environ. Sci. Technol. 43, 2937-2942.

Yan, W., Jing, C., 2014. Sorption behavior of organophosphate esters on carbon nanotubes with different surface oxidation. Environ. Chem. 33, 1692-1699.

Yuan, X., Lacorte, S., Cristale, J., Dantas, R.F., Sans, C., Esplugas, S., Qiang, Z., 2015. Removal of organophosphate esters from municipal secondary effluent by ozone and UV/H_2O_2 treatments. Sep. Purif. Technol. 156, 1028-1034.

Yujia, C., Jinshao, Y., Ya, C., Han, H., Hongling, Z., Huase, O., 2019. Degradation kinetics, mechanism and toxicology of tris(2-chloroethyl) phosphate with 185 nm vacuum ultraviolet. Chem. Eng. J. 356, 98-106.

Zhou, C., Gao, N., Deng, Y., Chu, W., Rong, W., Zhou, S., 2012. Factors affecting ultraviolet irradiation/hydrogen peroxide (UV/H_2O_2) degradation of mixed N-nitrosamines in water. J. Hazard. Mater. 231-232, 43-48.

Figure Captions

Fig.1. The degradation efficiency and kinetics of TCPP from 0 to 900 min in the UV/H_2O_2 system (C_{TCPP}= 5 mg L^{-1}, C_{H2O2}=50 mg L^{-1}, P_{UV}=250 W)

Fig.2. The (A) TOC removal (B) pH values (C) Cl^- concentration and (D) PO_4^{3-} concentration of TCPP from 0 to 900 min in the UV/H_2O_2 system (C_{TCPP}= 5 mg L^{-1}, C_{H2O2}=50 mg L^{-1}, P_{UV}=250 W)

Fig.3. Two pathways of TCPP (A and B)

Fig.4. Luminescence inhibition rate of degraded TCPP for 20 times diluted and 100 times diluted

Table 1

The frontier electron densities and bond dissociation enthalpies

Atom	FED_{HOMO}^2	FED_{LUMO}^2	$2FED_{HOMO}^2$	$FED_{HOMO}^2 + FED_{LUMO}^2$
P1	0.010	0.878	0.021	0.888
O2	0.007	0.140	0.014	0.147
O3	0.006	0.267	0.011	0.273
C4	0.001	0.179	0.001	0.180
C5	0.001	0.370	0.002	0.371
Cl 6	0.000	0.259	0.001	0.259
O7	0.001	0.412	0.003	0.414
O8	0.106	0.041	0.212	0.147
C9	0.172	0.013	0.344	0.185
C10	0.001	0.083	0.002	0.084
C11	0.000	0.496	0.001	0.496
Cl 12	0.000	0.344	0.000	0.344
C13	0.000	0.028	0.000	0.028
C14	0.002	0.041	0.004	0.043
C15	0.295	0.025	0.591	0.321
Cl 16	0.174	0.006	0.349	0.180
C17	0.007	0.001	0.013	0.008

Table 2

Bond energy in TCPP

Bonds	Bond energy
P1-O2	1.5388
P1-O3	0.8370
P1-O7	0.8192
P1-O8	0.6216
O3-C4	0.9151
C4-C5	0.9787
C5-Cl 6	0.9395
C4-C13	1.0036
O7-C10	0.9066
C10-C11	0.9793
C11-Cl 12	0.9435
O8-C9	1.1589
C9-C15	0.6844
C15-Cl 18	0.9685
C9-Cl 17	0.9685
C10-C14	1.0041
C15-Cl 16	0.9685

Table 3

The intermediate products of TCPP in the UV/H_2O_2 system

No.	t_R (min)	Name	Toxicity LD_{50} (Rat,oral)	EI-MS spectrum ions	Possible structure
1	8.08	(*Z*)-1-chloroprop-1-ene	221 mg L^{-1} (LC_{50}, mouse, inhalation)	41 (999); 39 (741); 76 (390); 38 (153); 78 (128); 40 (114); 37 (110); 49 (73); 75 (51uk); 27 (50)|	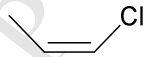
2	8.63	Propane-1,2-diol	20000 mg kg^{-1}	207 (999); 147 (816); 298 (762); 73 (611); 283 (237); 208 (209); 299 (196); 209 (150); 135 (139); 133 (133)	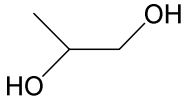
3	9.85	2-hydroxypropanoic acid	3543 mg kg^{-1}	73 (999); 117 (696); 147 (691); 45 (182); 75 (142); 191 (126); 66 (122); 148 (112); 190 (99); 74 (92)	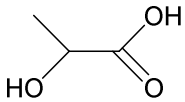
4	9.19	Oxalic acid	7500 mg kg^{-1}	147 (999); 73 (924); 148 (165); 45 (150); 74 (88); 149 (84); 66 (80); 72 (69); 190 (65); 59 (58)	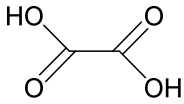

5	26.72	Triisopropyl phosphate	NA	99 (999); 125 (682); 43 (354); 41 (183); 141 (160); 45 (153); 27 (87); 123 (76); 42 (74); 39 (70)	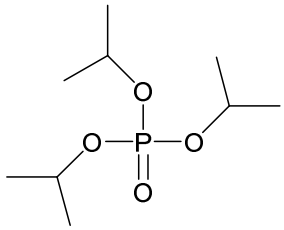
6	19.06	Diisopropyl hydrogen phosphate	NA	99 (999); 125 (585); 41 (478); 43 (337); 42 (287); 91 (283); 65 (155); 45 (103); 40 (90); 139 (84)	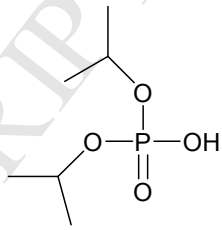
7	7.41	Propan-2-ol	5045 mg kg^{-1}	147 (999); 75 (864); 73 (745); 45 (301); 117 (265); 43 (249); 131 (169); 133 (163); 148 (145); 59 (143)	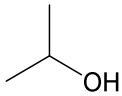
8	8.96	Phosphorous acid	NA	207 (999); 147 (816); 298 (762); 73 (611); 283 (237); 208 (209); 299 (196); 209 (150); 135 (139); 133 (133)	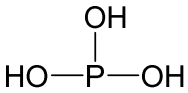
9	14.62	Phosphoric acid	1530 mg kg^{-1}	299 (999); 73 (464); 300 (252); 314 (184); 301 (132); 45 (112); 133 (84);	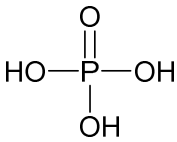

				211 (64); 75 (52); 147 (52)	
10	20.04	1-hydroxypropan-2-yl dihydrogen phosphate	NA	73 (999); 18 (601); 299 (441); 256 (220); 75 (184); 211 (181); 117 (157); 45 (145); 17 (138); 227 (133)|	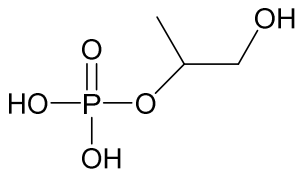
11	23.20	Bis(1-hydroxypropan-2-yl) hydrogen phosphate	NA	73 (999); 131 (267); 227 (204); 211 (199); 75 (188); 130 (184); 285 (160); 299 (152); 117 (130); 115 (118)	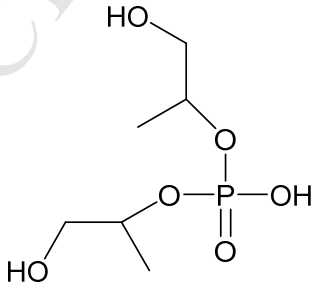

*Most of the toxicity data were obtained from Wikipedia (http://en.wilipedia.org/wiki/); NA means the toxicity data are not available.

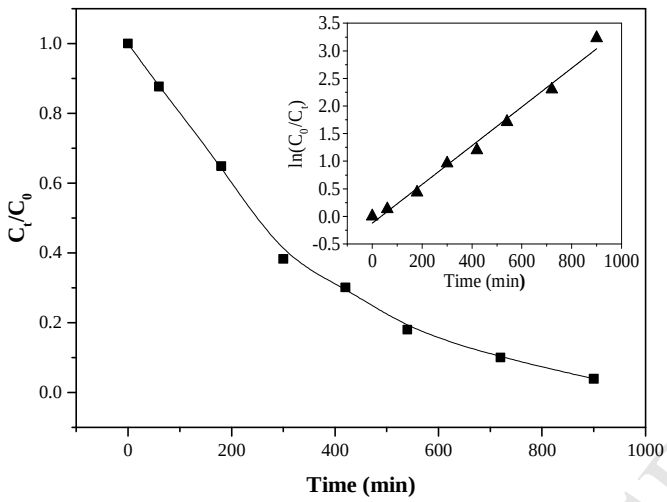

Fig.1. The degradation efficiency and kinetics of TCPP from 0 to 900 min in the UV/H_2O_2 system (C_{TCPP}= 5 mg L^{-1}, C_{H2O2}=50 mg L^{-1}, P_{UV}=250 W)

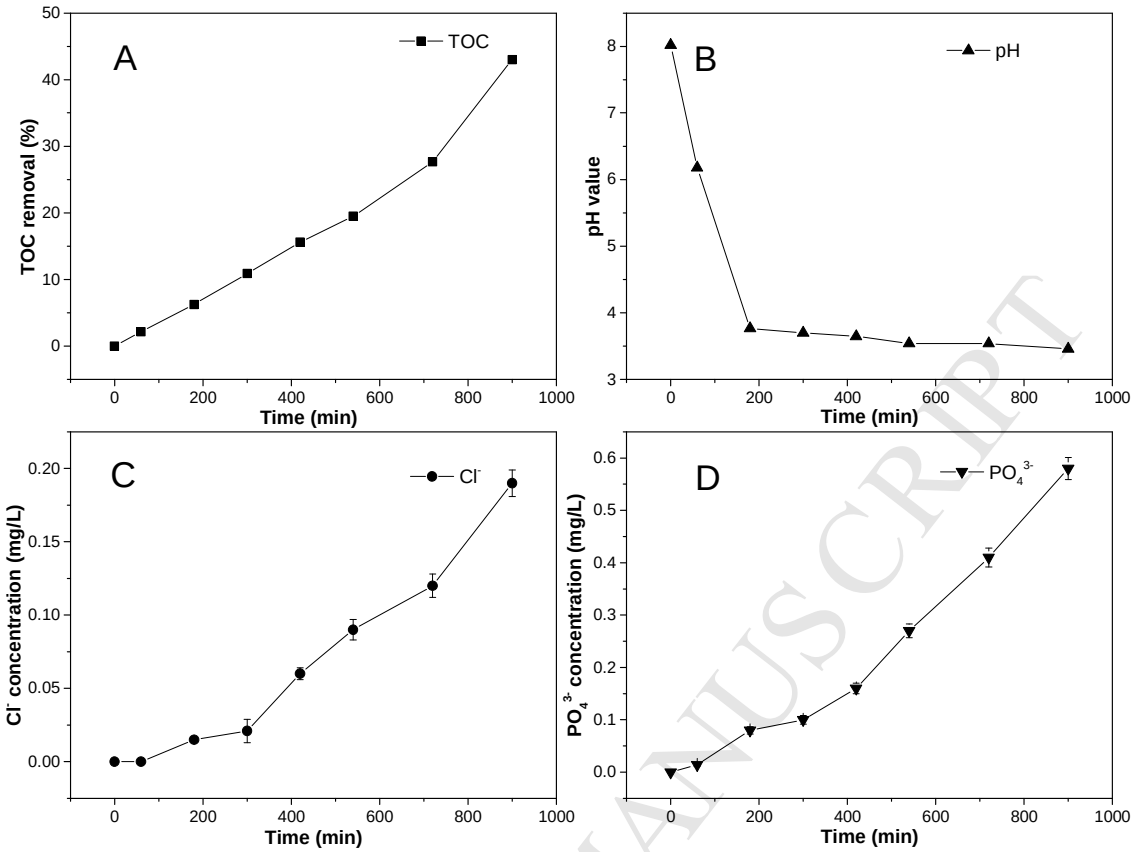

Fig.2. The (A) TOC removal (B) pH values (C) Cl^- concentration and (D) PO_4^{3-} concentration of TCPP from 0 to 900 min in the UV/H_2O_2 system (C_{TCPP}= 5 mg L^{-1}, C_{H2O2}=50 mg L^{-1}, P_{UV}=250 W)

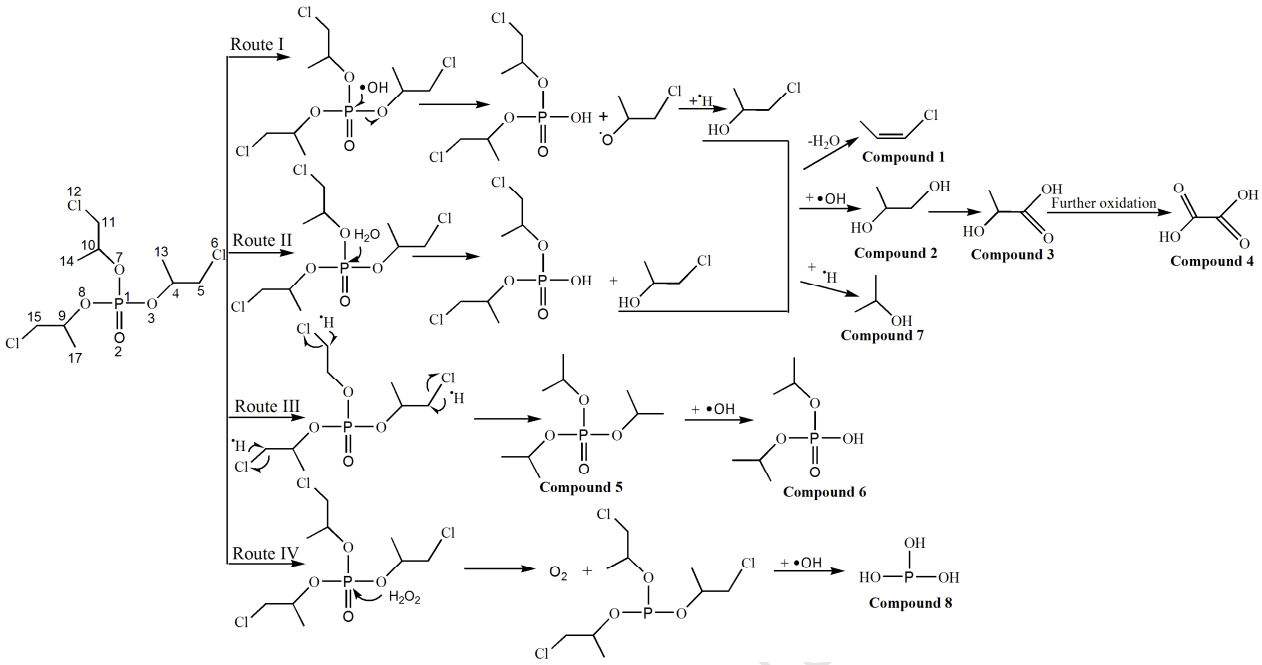

(A)

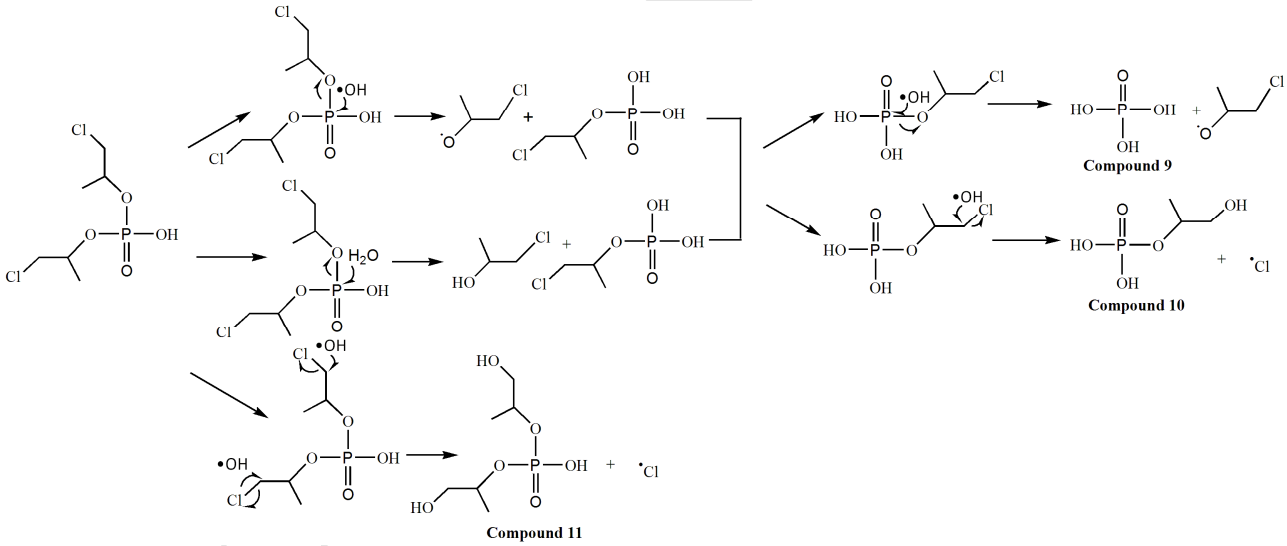

(B)

Fig.3. Two pathways of TCPP (A and B)

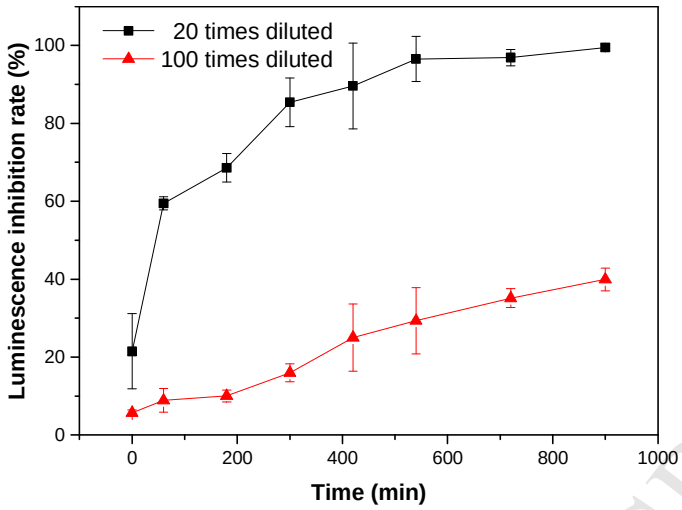

Fig.4. Luminescence inhibition rate of degraded TCPP for 20 times diluted and 100 times diluted

- UV/H_2O_2 system is an effective method to degrade TCPP in aqueous solution.
- TCPP was transformed to several hydroxylated and dechlorinated products.
- The degradation products of high concentration TCPP were more toxic.